Posted on 5 Dec 2022 — The copyright holder is the author/funder. All rights reserved. No reuse without permission. — https://doi.org/10.22541/au.167024883.31459211/v1 — This a preprint and has not been peer reviewed. Data may be preliminary.

Dexamethasone changes the disposition of atorvastatin by targeting the LXRα-OATP1B1 pathway

Xiaochun Li[1], Daqiang Zhan[1], Yuanzhi Wang[1], Yidan Gou[1], Shijiao Cai[1], Jingyue Zhang[1], Yifan He[1], Ruiting Zhao[1], Ye Tian[1], Rongcai Jiang[1], and Hengjie Yuan[1]

[1]Tianjin Medical University General Hospital

December 5, 2022

Abstract

Chronic subdural hematoma (CSDH) is one of the most common neurological disorders. In recent years, atorvastatin (ATV) combined with dexamethasone (DXM) has been proved to be a more efficacious therapy in treating patients with CSDH than ATV monotherapy. To investigate whether DXM has an effect on the pharmacokinetics of ATV, the expression of organic anion transport polypeptides 1B1 (OATP1B1) and upstream nuclear receptors liver X receptor α (LXRα) in rat liver and HepG2 cells were evaluated. The results showed that when DXM was combined with ATV, the area under curve (AUC(0˜[?])) of ATV, o-ATV and p-ATV was increased by 1.550, 1.420, 1.676 times, respectively. In HepG2 cells, DXM inhibited the uptake of ATV by 59.24%. Also, DXM decreased the expression of OATP1B1 and LXRα both in the rat liver and HepG2 cells. Dual-luciferase reporter assay indicated that DXM had an inhibitory effect on the LXRα-OATP1B1 pathway. In conclusion, DXM downregulated the protein expression of OATP1B1 by inhibiting the LXRα-OATP1B1 pathway, thus, decreasing hepatic drug uptake and increasing plasma concentration of ATV and its active metabolites.

Δεξαμετηασονε ςηανγες τηε δισποσιτιον οφ ατοραστατιν βψ ταργετινγ τηε ΛΞΡα-ΟΑΤΠ1Β1 πατηωαψ

Xiaochun Li[1,2#], Daqiang Zhan[1,3#], Yuanzhi Wang[1,4#], Yidan Gou[1], Shijiao Cai[1], Jingyue Zhang[1], Yifan He[1], Ruiting Zhao[1], Ye Tian[5], Rongcai Jiang[5], Hengjie Yuan[1*]

[1] Tianjin Medical University, Department of Pharmacy, Tianjin Medical University General Hospital, Tianjin, 300052 China.

[2] Department of Pharmacy, Wanping Community Health Care Center, Beijing, 100165 China.

[3] Department of Pharmacy, Second Affiliated Hospital of Hainan Medical University, Hainan, 570216 China.

[4] Department of Pharmacy, The Sixth Hospital of Shanxi Medical University, Taiyuan, 030008 China.

[5] Department of Neurosurgery, Tianjin Medical University General Hospital, Tianjin Medical University, Tianjin 300052, China

*Correspondence: hengjieyuan@163.com.

# Xiaochun Li, Daqiang Zhan and Yuanzhi Wang contributed equally to this work.

Acknowledgements

The authors acknowledge the role of all support staff in the study.

Authors' contributions

Posted on 5 Dec 2022 — The copyright holder is the author/funder. All rights reserved. No reuse without permission. — https://doi.org/10.22541/au.167024883.31459211/v1 — This a preprint and has not been peer reviewed. Data may be preliminary.

HJY, YT, RCJ, DQZ, and XCL contributed substantially to the collection of literature, the study design, the data interpretation. XCL and SJC performed the writing of the manuscript. DQZ and XCL contributed to the acquisition of data. DQZ performed the pharmacokinetics of drugs and methodology of LC-MS/MS. XCL completed the cerebrospinal fluid collection part of experiment and cell culture. DQZ, JYZ, XCL and YZW performed mass spectrometry. RTZ, YFH and YDG provided their suggestions in this study. All authors read and approved the final manuscript.

Funding

This work was supported by Grants of the National Natural Science Foundation of China [grant numbers 81971173, 81501057, 81102447]; Tianjin Municipal Science and Technology Commission [grant number 16JCQNJC10600]; Science Project of Tianjin Municipal Educational Commission [grant number 2019ZD032]. The funders had no role in study design; in the collection, analysis and interpretation of data; in the writing of the report; and in the decision to submit the article for publication.

Conflict of interest statement

The authors have no conflicts of interest to declare.

Abstract

Chronic subdural hematoma (CSDH) is one of the most common neurological disorders. In recent years, atorvastatin (ATV) combined with dexamethasone (DXM) has been proved to be a more efficacious therapy in treating patients with CSDH than ATV monotherapy. Our recent study found that ATV in hematoma fluid was higher in patients receiving ATV combined with DXM, as compared to those receiving ATV monotherapy. However, the underlying mechanism of how DXM improves the level of ATV is not yet clear. The purpose of this study was to investigate the effects of DXM on pharmacokinetics of ATV and the expression of organic anion transport polypeptides 1B1 (OATP1B1) and upstream nuclear receptors liver X receptor α (LXRα) in rat liver and HepG2 cells were evaluated. The results showed that when DXM was combined with ATV, the area under curve ($AUC_{(0\text{-}[?])}$) of ATV, *o*- ATV and*p*- ATV was increased by 1.550, 1.420, 1.676 times, respectively. In HepG2 cells, DXM inhibited the uptake of ATV by 59.24%. Also, DXM decreased the expression of OATP1B1 and LXRα both in the rat liver and HepG2 cells. Dual-luciferase reporter assay indicated that DXM had an inhibitory effect on the LXRα-OATP1B1 pathway. In conclusion, DXM downregulated the protein expression of OATP1B1 by inhibiting the LXRα-OATP1B1 pathway, thus, decreasing hepatic drug uptake and increasing plasma concentration of ATV and its active metabolites.

Keywords: atorvastatin, dexamethasone, disposition, LXRα, OATP1B1

Abbreviations

ATV, atorvastatin; $AUC_{(0\text{-}t)}$, area under plasma concentration-time curve from time 0 to 24 hours; $AUC_{(0\text{-}[?])}$, area under plasma concentration-time curve from time 0 to infinity; C_{max}, peak plasma concentration; CSDH, chronic subdural hematoma; CSF, cerebrospinal fluid; DXM, dexamethasone; LXRα, liver X receptor α· LC-MS/MS, liquid chromatogram-mass spectrometer/ mass spectrometer; LLOQ, the lower limit of quantification; OATP1B1, organic anion transporting polypeptides;*o*- ATV*, o*- hydroxy atorvastatin calcium; *p*- ATV*, p*- hydroxy atorvastatin calcium; RSV, rosuvastatin; t_{max}, time to peak plasma concentration; and $t_{1/2}$, elimination half-life.

1.Introduction

Chronic subdural hematoma (CSDH) is one of the most common neurological disorders and is particularly prevalent among elderly patients[1]. Surgical evacuation is often the main management for symptomatic patients or hematomas exerting a significant mass effect. Although most of the patients showed good results from surgical treatment, however, some patients had a post-operative recurrence and the recurrence rate was up to 33%[2]. The incidence of CSDH is increasing along with the continuous development of the aging society. Therefore, it is significantly important to investigate the effective non-surgical treatment of CSDH[3].

Posted on 5 Dec 2022 — The copyright holder is the author/funder. All rights reserved. No reuse without permission. — https://doi.org/10.22541/au.167024883.31459211/v1 — This a preprint and has not been peer reviewed. Data may be preliminary.

Meta-analysis comparing the effectiveness of different drug treatments in improving recurrence in patients with CSDH has shown that atorvastatin (ATV), dexamethasone (DXM), and tranexamic acid are efficient in improving recurrence in CSDH patients, and among them, ATV combined with DXM is the best intervention for CSDH[4]. One phase II randomized proof of concept clinical trial confirmed that low-dose DXM combined with ATV was more effective than ATV alone in reducing hematoma volume and improving neurological function in patients with CSDH[5]. Thus, the combination of DXM with ATV can inhibit vascular leakage caused by inflammatory reactions and avoid the long-term use of drug-induced adverse effects[6]. These studies suggested that there may have potential drug-drug interactions between DXM and ATV, which produced a synergistic effect in the treatment of CSDH.

Our previous study has demonstrated that DXM can enhance the anti-inflammatory and -angiogenic activities of ATV by increasing the ATV level in hematoma fluid and serum and by regulating the functions of macrophages[7]. However, the underlying mechanism of how DXM increases the presence of ATV in hematoma fluid and serum is still unknown. Therefore, we proposed the hypothesis that DXM increased the plasma concentration of ATV by inhibiting the expression of transporter. Organic anion transport polypeptides 1B1 (OATP1B1) is a transporter particularly expressed on the sinusoidal membrane of hepatocytes and mediates the uptake of drugs from blood into hepatocytes[8]. Meanwhile, inhibitors of OATP1B1 such as gemfibrozil can increase the plasma concentrations of ATV and its metabolites by about 1.5-fold, which suggests that OATP1B1 plays an essential role in drug-drug interactions of ATV[9]. Liver X receptor α (LXRα) regulates the transcription of OATP1B1 in liver-derived cell lines[10]. In addition, drug concentration analysis in vivo is the most direct and effective method to study drug pharmacokinetics and investigate drug-drug interactions. Meanwhile, LC-MS/MS is one of the most used analytical methods in the evaluation of ATVs for its better qualitative and quantitative capacities and higher resolution[11]. In our study, we investigated the effects of DXM on the pharmacokinetics of ATV and its active metabolites in rat plasma, and the distribution of ATV in cerebrospinal fluid and HepG2 cells based on the LC-MS/MS method for the detection of ATV and its active metabolites in rat plasma. The expression of OATP1B1 and its upstream nuclear receptors LXRα were also evaluated to investigate the underlying mechanism.

2.Methods

2.1 Chemicals and Reagents

Atorvastatin calcium tablet was provided by Pfizer (USA). Dexamethasone acetate tablet was provided by Xinyi (China). Atorvastatin calcium (ATV, 99.4% purity), *o*- hydroxy atorvastatin calcium (*o*- ATV, 97.6% purity), and *p*- hydroxy atorvastatin calcium (*p*- ATV, 98.7% purity) were all supplied by TLC PharmaChem company (Canada). Meanwhile, d5-atorvastatin calcium (d5-ATV, 96% purity, 99.5% isotopic content) was purchased from Toronto Research Chemicals Company (Canada). Rosuvastatin (RSV, 98% purity) was obtained from Solarbio (China). GW3965 was provided by Selleck (USA). Moreover, the Dual-luciferase reporter assay system was purchased from Yeasen (China). Furthermore, Lipofectamine 3000 was purchased from Thermo Fisher Scientific (USA).

2.2 Animals

Male Sprague-Dawley (SD) rats (250 g ± 10 g) were purchased from Beijing HFK Biotechnology Co., Ltd (Beijing, China). All rats were kept and maintained in the animal facility of Tianjin Medical University General Hospital under a 12-h light/dark cycle in a temperature-controlled room (25 ± 3 °C) with free access to clean food and water and were adapted to the environment for a week before the experiments.

The study was conducted in accordance with the Basic & Clinical Pharmacology & Toxicology policy for experimental and clinical studies[12]. All experimental procedures involving the animals were reviewed and approved by the Tianjin Medical University Animal Ethics Committee (Tianjin, China).

2.3 Drug treatment

A total of 24 rats were randomly assigned to the following four groups: control group, ATV group, DXM group, and ATV+DXM group. Based on the oral dosage of CSDH patients, the dose for rats is 0.27 mg/100

Posted on 5 Dec 2022 — The copyright holder is the author/funder. All rights reserved. No reuse without permission. — https://doi.org/10.22541/au.167024883.31459211/v1 — This a preprint and has not been peer reviewed. Data may be preliminary.

g atorvastatin calcium and 0.02 mg/100 g dexamethasone acetate, which were administered via oral gavage daily.

2.4 Plasma, cerebrospinal fluid, and liver

Blood samples (1–1.2 mL) were collected from each rat through the epicanthal vein at 15 min, 35 min, 1 h, 1.5 h, 2 h, 3 h, 4 h, 6 h, 8 h, 12 h, and 24 h after drug administration to investigate the effect of DXM on the pharmacokinetics of ATV and its metabolites. Then, plasma was separated from the blood by centrifugation (3500 rpm for 10 minutes at 4) and EDTA-K2 was used as the anticoagulant agent. On the 5th day of gavage administration, the animals were anesthetized with 7% chloral hydrate after oral dosing for 1 h. Based on the literature[13], a venous blood collection needle and a 1mL syringe with the needle removed were assembled, which was used to collect cerebrospinal fluid (CSF) of about 100 μL from the cisterna magna. If CSF is mixed with blood, it can be centrifuged at 4 , 10000 rpm for 2 minutes, and then take the supernatant. In addition, the CSF and plasma samples were stored at -80 and -20 , respectively, which were used to measure the drug concentration by LC-MS/MS later. After taking CSF and blood, the rat was perfused with ice PBS until the liver color changes from red to earthy yellow, and then the liver was excised, weighed, and stored at -80 until analysis.

2.5 Cell culture and drug treatments

The human liver carcinoma cell line HepG2 was provided by Tianjin Medical University General Hospital (Tianjin, China). The cells were seeded in 6-well plates (Corning, USA) at a density of 7.5×10^4 cells/well and cultured in the Dulbecco's modified Eagle medium (Gibco, USA) supplemented with 10% fetal bovine serum (Biological Industries, Israel) and 1% penicillin/streptomycin in a 5% CO_2 humidified incubator at 37 °C. Based on our previous study, the ATV and DXM steady-state concentration in rat plasma was 26–125 nM, and 280–400 nM, respectively when the rats were orally administered with 0.27 mg/100g ATV and 0.02 mg/100g DXM. Thus, HepG2 cells were treated with 0.1% DMSO, 100 nM ATV, 400 nM DXM, 100 nM ATV, and 400 nM DXM for 3 days. Meanwhile, Cell Counting Kit-8 was used to detect the cytotoxicity of 100 nM ATV and 400 nM DXM on HepG2 cells following the manufacturer's protocol. Finally, absorption intensity was measured at 450 nm using a microplate reader (Thermo, USA).

2.6 Quantification of the concentration of ATV and its metabolites by LC-MS/MS

ATV, ortho-hydroxy-atorvastatin (*o*- ATV), and para-hydroxy-atorvastatin (*p*- ATV) in plasma and CSF were extracted with ethyl acetate. Cell samples were processed with acetonitrile for protein precipitation before LC-MS/MS. Then, the Waters ACQUITY UPLC I-Class system (Waters, USA) equipped with an Acquity UPLC BEH C18 column (1.7 μm, 100 × 2.1 mm, Waters, USA) was coupled online to a Waters Xevo TQD IVD triple quadrupole mass spectrometer (Waters, Ireland) with electrospray ionization and multiple reaction monitoring in positive ion mode. The mobile phase consisted of solvent A (acetonitrile with 0.01% formic acid) and solvent B (0.01% aqueous formic acid) with a gradient elution of 0.0 min, 80%B; 1.0 min, 60%B; 4 min, 10%B; 4.5 min, 90%B; 4.51 min, 80%B; and 5 min, 80%B. The flow rate and the injection volume were 0.4 mL/min and 10 μL, respectively. Data acquisition was performed by Masslynx (Version 4 1, Waters, USA).

2.7 Western blot assay

Proteins were extracted with a radio-immunoprecipitation assay (RIPA) buffer containing phenylmethane sulfonyl fluoride (Sigma, St. Louis, MO, USA) and a protease inhibitor cocktail (Sigma). Herein, protein concentration was determined using the bicinchoninic acid assay (BCA, Thermo). Then, proteins were separated by 10% SDS-PAGE and then transferred to polyvinylidene difluoride (PVDF) membranes. Subsequently, the membranes were incubated with primary antibodies at 4 °C overnight. The primary antibodies used were as follows: anti-OATP1B1(1:1000 dilutions; Santa Cruz Biotechnology, Santa Cruz, USA), anti-LXRα (1:500 dilutions; Santa Cruz Biotechnology, Santa Cruz, USA), and anti-β-actin (1:2000 dilutions; ZSGB-BIO, Beijing, China). Then, the membranes were incubated with appropriate horseradish peroxidase (HRP)-conjugated secondary antibody at room temperature for 1 h and visualized using electrochemilumi-

Posted on 5 Dec 2022 — The copyright holder is the author/funder. All rights reserved. No reuse without permission. — https://doi.org/10.22541/au.167024883.31459211/v1 — This a preprint and has not been peer reviewed. Data may be preliminary.

nescence (ECL) HRP substrate. Meanwhile, signals of antibody binding were detected by Gensye automatic gel imaging analysis system. Relative protein levels were standardized with the β-actin protein level and protein band intensities were analyzed by ImageJ (National Institutes of Health, Bethesda, MD).

2.8 Dual-luciferase reporter assay

pGL3-OATP1B1, pTracer-hLXRα, and internal reference Renilla luciferase plasmid pRL-TK vector were purchased from Tsingke (Nanjing, China). The direct binding of LXRα to the OATP1B1 5'UTR was described in previous research containing LXRα response element (-128 to + 53 bp)[10]. Herein, HepG2 cells were seeded in 6-well plates at a density of 7.5×10^4 cells/well. After 24 hours, the cells were transfected with corresponding plasmids with Lipofectamine 3000 transfection reagent following the manufacturer's protocol. The empty pTracer plasmid was used as a control. Afterward, cells were incubated by 0.1% DMSO, 400 nM DXM, 10 μM GW3965, or 400 nM DXM combined with 10 μM GW3965 for 3 days. Finally, the cells were processed using the dual-luciferase reporter assay system (Yeasen, Shanghai, China) based on the manufacturer's protocol.

2.9 Statistical analysis

Pharmacokinetic parameters were estimated from plasma concentration data via non-compartmental analysis using the professional pharmacokinetic software DAS 3.0 (Drug and statistics software 3.0). The experimental data were presented as mean ± SD or median (25^{th}–75^{th} percentile), depending on a normal or skewed distribution of data determined by the Shapiro-Wilk test. GraphPad Prism 9.0 was used to perform statistical analyses. Comparisons between the two groups were tested by a two-tailed Student's t-test or Mann-Whitney U test based on the distribution of data. The difference among multiple groups was evaluated by one-way analysis of variance (one-way ANOVA). Statistical significance was defined as $P < 0.05$.

3.Results

3.1 Methodology of LC-MS/MS

The representative chromatograms of ATV, *o*- ATV, *p*- ATV, d5-ATV, and RSV were shown in Figure 1. The retention times of ATV,*o*- ATV, *p*- ATV, d5-ATV, and RSV were 3.06 min, 2.78 min, 1.81 min, 3.05 min, and 1.83 min, respectively. In addition, the standard curves of ATV, *o*- ATV, and *p*- ATV all showed good linearity over the concentration range of 0.082–50 ng/mL. The regression equation was listed in Table1. Meanwhile, the correlation coefficient (r^2) was all above 0.99. Moreover, the lower limit of quantification (LLOQ) of ATV, *o*- ATV, and*p*- ATV was 0.082 ng/mL.

The results of intra- and inter-batch precision and the accuracy of ATV,*o*- ATV, and *p*- ATV were listed in Table 2. The precision and accuracy variation were all less than 15%, which indicated that the precision and accuracy were satisfactory.

Herein, matrix effect (MF) values (%) of ATV at high-quality control (HQC) and low-quality control (LQC) concentrations were 106.6 ± 6.5 and 106.5 ± 6.1, respectively; *o*- ATV at HQC and LQC concentrations were 95.9 ± 11.3, 105.3 ± 7.4, respectively; and *p*- ATV at HQC and LQC concentrations were 89.8 ± 8.9, 90.1 ± 6.8, respectively. The MF variations were all less than 15%, which suggested that there were few matrix effects. The HQC, middle-quality control (MQC), and LQC extraction recoveries of the ATV were 91.7%, 100.8%, and 93.20%, respectively; *o*- ATV were 71.2%, 70.01%, and 69.2%; and*p*- ATV were 87.1%, 77.48%, and 75.1%. MF values and extraction recovery values were listed in Tables 3 and 4.

The results of the analytes' stability were displayed in Table 5. ATV,*o*- ATV, and *p*- ATV were all stable and had no significant degradation observed in rat plasma under different conditions (4 h at room temperature, 24 h in autosampler, 24 h in 4 refrigerator, and 36 days in a -20 refrigerator).

3.2 Effects of DXM on the pharmacokinetics of ATV and its metabolites in rats

After a single oral dose of ATV with or without DXM, the plasma concentrations of ATV, *o*- ATV, and *p*- ATV at each time point were determined, as presented in Figure 2. Meanwhile, the pharmacokinetic

parameters of ATV, *o*- ATV, and *p*- ATV are presented in Table 6. Herein, DXM increased the plasma exposure of ATV substantially. Compared with ATV alone, the C_{max} (peak plasma concentration) of ATV was increased by 0.388 times with DXM, and the $AUC_{(0\text{-}t)}$ and $AUC_{(0\text{-}[?])}$ were increased by 1.156 times ($P < 0.05$) and 1.550 times ($P< 0.05$), respectively. Moreover, the $AUC_{(0\text{-}t)}$and $AUC_{(0\text{-}[?])}$ values of the two active metabolites*o*- ATV and *p*- ATV were increased with DXM, although there were no statistical differences found in the C_{max}values, which were only slightly increased by 0.313 times and 0.106 times, respectively. $AUC_{(0\text{-}t)}$ and $AUC_{(0\text{-}[?])}$ of *o*- ATV were increased by 1.320 times ($P < 0.05$) and 1.420 times ($P < 0.05$), respectively. Furthermore, the corresponding values for *p*- ATV were increased by 1.209 times ($P < 0.05$) and 1.676 times ($P < 0.05$), respectively. The t_{max} (time to peak plasma concentration) remained statistically unaltered by DXM, for atorvastatin and its active metabolites. DXM lengthened the $t_{1/2}$ (elimination half-life) of ATV, *o*- ATV, and *p*- ATV by 1.304 times ($P < 0.05$), 1.196 times ($P < 0.05$), and 1.457 times ($P < 0.05$), respectively.

3.3 ATV cannot cross the blood-brain barrier into CSF

After 5 days of oral administration of ATV with or without DXM, the concentrations of ATV in plasma and CSF at the same time point were determined. Based on our pharmacokinetics results, drug concentration after oral administration of 24 and 1 h was defined as valley concentration and peak concentration, respectively. As shown in Figure 3, the valley and peak concentrations of ATV in CSF were all below 0.5 ng/mL. However, this was not the same case in plasma. In the ATV group, valley concentration in plasma was distributed from 0.1234 to 0.3476 ng/mL, and peak concentration in plasma was distributed from 2.952 to 23.29 ng/mL. Meanwhile, in the ATV+DXM group, valley concentration in plasma was distributed from 0.0904 to 0.9449 ng/mL, and peak concentration in plasma was distributed from 21.08 to 63.47 ng/mL. However, no matter if it was a valley or peak concentration, the level of ATV in CSF was lower than in plasma ($^*P < 0.05$, $^{**}P < 0.01$). In addition, comparing the peak concentration of ATV between the ATV group and the ATV+DXM group, DXM significantly increased the ATV level in plasma ($^*P < 0.05$), which was consistent with the pharmacokinetic results. Therefore, these results suggested that ATV cannot cross the blood-brain barrier into CSF.

3.4 ΔΞΜ ινηιβιτεδ τηε εξπρεσσιον οφ ΟΑΤΠ1Β1 ανδ ΛΞΡα ιν ρατ λιερ

Herein, we first detected the effect of ATV and DXM on the expression of OATP1B1. Compared with the control and ATV groups, the protein levels of OATP1B1 were significantly decreased in the DXM and ATV+DXM groups (Figures 4A and B, $^*P < 0.05$, $^{**}P < 0.01$). Literature suggests that the expression of OATP1B1 can be upregulated when nuclear receptors LXRα are activated [10, 14]. Thus, LXRα protein expression was also decreased in DXM and ATV+DXM groups, compared with the control and ATV groups (Figures 4C and D, $^{**}P < 0.01$, $^{***}P < 0.001$). These results indicated that DXM has an inhibitory effect on OATP1B1 and the upstream nuclear receptor LXRα in rat liver.

3.5 ΔΞΜ δεςρεασεδ τηε υπτακε οφ ΑΤ″ ανδ ινηιβιτεδ ΟΑΤΠ1Β1 ανδ ΛΞΡα εξπρεσσιονς ιν ΗεπΓ2 ςελλς

HepG2 cells were treated with 100 nM ATV and 400 nM DXM for 3 days to verify the effects of DXM on OATP1B1 transport function in HepG2 cells and the underlying mechanism. The CCK-8 assay showed that 100 nM ATV and 400 nM DXM had no cytotoxicity in HepG2 cells (Figure 5A). We found that in the ATV group, the uptake of ATV by HepG2 cells was 5.307 ± 0.5764 ng/mL, and in the ATV+DXM group was 2.163 ± 0.3038 ng/mL by measuring the ATV concentration in cell lysis through LC-MS/MS. Compared with the ATV group, the concentration of ATV was decreased by 59.24% in the ATV+DXM group (Figure 5B, $^{**}P < 0.01$). These results can explain the increasing concentration of ATV in plasma. Compared with the control and ATV groups, the protein expressions of OATP1B1 and LXRα were decreased in the DXM and ATV+DXM groups (Figures 5C–E, $^*P< 0.05$). Therefore, DXM could suppress ATV uptake in HepG2 cells and DXM may downregulate the protein expression of OATP1B1 via LXRα.

3.6 ΔΞΜ ινηιβιτεδ ΟΑΤΠ1Β1 προμοτερ αςτιατιον ια ΛΞΡα

Ποστεδ ον 5 Δες 2022 . Τηε ςοπψριγητ ηολδερ ις τηε αυτηορ/φυνδερ. Αλλ ριγητς ρεσερϖεδ. Νο ρευσε ωιτηουτ περμισσιον. , ηττπς://δοι.οργ/10.22541/αυ.167024883.31459211/1 . Τηις α πρεπριντ ανδ ηας νοτ βεεν πεερ ρεϖιεωεδ. Δατα μαψ βε πρελιμιναρψ.

Posted on 5 Dec 2022 — The copyright holder is the author/funder. All rights reserved. No reuse without permission. — https://doi.org/10.22541/au.167024883.31459211/v1 — This a preprint and has not been peer reviewed. Data may be preliminary.

In addition, the 5' UTR of the OATP1B1 DNA containing the LXRα response element was cloned into the pGL3 vector to assess the effect of DXM on LXRα-mediated OATP1B1 promoter activation. The activity of the firefly luciferase was monitored after incubation by 400 nM DXM or LXRα agonist GW3965 as a positive control. As shown in Figure 6, the reporter activity was increased by 74% in the GW3965 group (****$P<$ 0.0001) and decreased by 33% in the DXM group (***$P<$ 0.001) as compared with 0.1% DMSO negative control. Meanwhile, compared with the GW3965 group, the DXM+GW3965 group also reduced the reporter activity by about 27% (****P < 0.0001). Thus, these results suggested that the repressive effect of DXM on the OATP1B1 expression was the result of the inhibition of OATP1B1 promoter activation via LXRα.

4.Discussion

ATV has been a widely used drug in the treatment of dyslipidemia and coronary heart disease for its cholesterol-lowering efficacy. However, beyond the hypolipidemic property, recent studies have also demonstrated that ATV has neuroprotective effects as the result of anti-inflammatory, antioxidant, and immunomodulatory activities[15-17]. Meanwhile, in our previous study[7], ATV can be detected in the hematoma fluid in CSDH patients and the concentration up to 40 ng/mL, thus raising the question of whether or not ATV can penetrate the blood-brain barrier (BBB). A hematoma is an encapsulated collection of fluid, blood, and blood degradation products layered between the arachnoid and dura mater. Moreover, it may create functional disruption of the BBB in CSDH patients[18, 19], which suggests that ATV in hematoma fluid may derive from CSF or blood. In this study, our results also showed that no matter how high the concentration of ATV in plasma, the ATV level in CSF was very low, nearly equivalent to zero, which indicated that ATV in plasma can hardly cross the BBB into CSF. ATV in hematoma fluid may originate from blood rather than CSF. The pathophysiological processes involved in the formation of CSDH showed that following the pathological delamination of the dural border cells, two membranes are formed and these membranes are the source of fluid exudation and hemorrhage, which contain numerous highly permeable capillaries[19]. Leaky capillaries under inflammatory stimulation may allow ATV derived from blood across the thin wall of capillaries into the hematoma fluid.

Therefore, the effect of DXM on the pharmacokinetics of ATV was investigated and then the effect of DXM on the uptake of ATV into hepatocytes was evaluated to investigate the underlying mechanisms of how DXM increased the ATV level in plasma. Our results showed that the combination of ATV and DXM increased the AUC of ATV, *o*- ATV, and*p*- ATV in plasma by 1.550, 1.420, and 1.676 times, respectively, and inhibited the uptake of ATV into hepatocytes by 59.24%. These results suggested that DXM changes ATV disposition by increasing ATV distribution in peripheral blood, which may be beneficial for ATV anti-inflammatory activity. As is known to all, ATV is an inhibitor of HMG-CoA reductase, which is the rate-limiting enzyme in cholesterol biosynthesis and the liver is the main site of its action[20]. However, collected pieces of evidence have suggested that statins have anti-inflammatory and antioxidant properties[21-23], which could be independent of their lipid-lowering activity. Kureishi et al. showed that simvastatin induced Akt-mediated phosphorylation of endothelial nitric oxide synthase, thereby leading to NO production, and promoting endothelial cell survival in an Akt-dependent manner. Thus, Akt may function as a new biological target for statin action[21]. In vitro, statins can downregulate receptors on macrophages that take up oxidized low-density lipoprotein, thus reducing the formation of foam cells[24]. Collectively, these pieces of evidence suggested that increasing ATV distribution in peripheral blood to a safe degree may be beneficial for ATV treatment of vascular inflammatory diseases.

In addition, ATV is the substrate of CYP3A4 and OATP1B1. Inhibitors of CYP3A4 and OATP1B1 combined with ATV could increase the plasma concentration of ATV to different degrees[25]. McCune et al[26] had shown that 2–250 μmol/L DXM can result in an average 1.7–6.9-fold increase in CYP3A4 activity in hepatocytes and DXM at doses used clinically can also increase CYP3A4 activity in vivo. However, our results showed that although DXM is a CYP3A4 inducer, DXM increased the AUC of ATV in plasma. Therefore, we speculated that DXM changes the plasma concentration of ATV and its metabolites *o*- ATV and*p*- ATV, which may be related to OATP1B1. Our study first provided evidence that OATP1B1 protein expression was downregulated by DXM. Meanwhile, OATP1B1 is highly expressed in the liver and localized

Posted on 5 Dec 2022 — The copyright holder is the author/funder. All rights reserved. No reuse without permission. — https://doi.org/10.22541/au.167024883.31459211/v1 — This a preprint and has not been peer reviewed. Data may be preliminary.

on the basolateral membrane of hepatocytes, which mediates the uptake of ATV from the portal vein into hepatocytes[27]. Therefore, the increased plasma concentrations of ATV and its active metabolites may be related to the inhibition of OATP1B1 by DXM. Moreover, the $t_{1/2}$of ATV and its two metabolites were prolonged by DXM, which could also be the result of less uptake of ATV into the liver when the expression of OATP1B1 was inhibited by DXM. These results were consistent with previous reports that green tea consumption enhanced hepatic CYP3A4 enzyme activity and lower OATP1B1 protein expression in rats, with an 85% and 93.3% increase in $AUC_{0–6h}$ of ATV and $AUC_{0–6h}$ of *o*- ATV[28].

LXRα is a member of the nuclear receptor superfamily and plays an important role in regulating target genes involved in drug metabolism and transport. We investigated the protein expression of LXRα and our results showed that DXM inhibited LXRα expression both in rat liver and human hepatocytes. In addition, dual-luciferase reporter assay showed that DXM inhibited OATP1B1 promoter activation via LXRα. However, whether or not DXM directly inhibited or downregulated the expression of LXRα through an intermediate substance remains to be further elucidated. In the human trophoblast cell line, DXM concentration dependently reduced the expression level of LXRα and the glucocorticoid receptor inhibitor could reverse dexamethasone-induced expression inhibitions of LXRα[29].

5.ὃνςλυσιον

Ιν τηις στυδψ, ωε προιδεδ ειδενςε τηατ ΔΞΜ ςομβινεδ ωιτη ΑΤ″ ςαν ινςρεασε τηε πλασμα ςονςεντρατιονς οφ ΑΤ″ ανδ ιτς αςτιε μεταβολιτες ανδ ρεδυςε ΑΤ″ λεελς ιν ηεπατοςψτες. Τηε ποτεντιαλ μεςηανισμ μαψ βε τηε ινηιβιτιον οφ τηε ΛΞΡα-OATP1B1 pathway by DXM. Increasing the distribution of ATV in peripheral blood may be beneficial for the treatment of CSDH.

References

1. Yang W, Huang J. Chronic Subdural Hematoma: Epidemiology and Natural History. Neurosurgery clinics of North America. 2017;28:205-10.

2. Uno M, Toi H, Hirai S. Chronic Subdural Hematoma in Elderly Patients: Is This Disease Benign? Neurologia medico-chirurgica. 2017;57:402-9.

3. Huang J, Gao C, Dong J, Zhang J, Jiang R. Drug treatment of chronic subdural hematoma. Expert opinion on pharmacotherapy. 2020;21:435-44.

4. Yu W, Chen W, Jiang Y, Ma M, Zhang W, Zhang X, et al. Effectiveness Comparisons of Drug Therapy on Chronic Subdural Hematoma Recurrence: A Bayesian Network Meta-Analysis and Systematic Review. Frontiers in pharmacology. 2022;13:845386.

5. Wang D, Gao C, Xu X, Chen T, Tian Y, Wei H, et al. Treatment of chronic subdural hematoma with atorvastatin combined with low-dose dexamethasone: phase II randomized proof-of-concept clinical trial. Journal of neurosurgery. 2020:1-9.

6. Zhang J. Expert consensus on drug treatment of chronic subdural hematoma. Chinese neurosurgical journal. 2021;7:47.

7. Gong Z, Zhan D, Nie M, Li X, Gao C, Liu X, et al. Dexamethasone enhances the efficacy of atorvastatin in inhibiting excessively inflammation-induced abnormal angiogenesis by regulating macrophages. J Neuroinflammation. 2021;18:203.

8. Liu X. SLC Family Transporters. Advances in experimental medicine and biology. 2019;1141:101-202.

9. Backman JT, Luurila H, Neuvonen M, Neuvonen PJ. Rifampin markedly decreases and gemfibrozil increases the plasma concentrations of atorvastatin and its metabolites. Clin Pharmacol Ther. 2005;78:154-67.

10. Meyer Zu Schwabedissen HE, Bottcher K, Chaudhry A, Kroemer HK, Schuetz EG, Kim RB. Liver X receptor alpha and farnesoid X receptor are major transcriptional regulators of OATP1B1. Hepatology

Posted on 5 Dec 2022 — The copyright holder is the author/funder. All rights reserved. No reuse without permission. — https://doi.org/10.22541/au.167024883.31459211/v1 — This a preprint and has not been peer reviewed. Data may be preliminary.

(Baltimore, Md). 2010;52:1797-807.

11. Kogawa AC, Pires A, Salgado HRN. Atorvastatin: A Review of Analytical Methods for Pharmaceutical Quality Control and Monitoring. Journal of AOAC International. 2019;102:801-9.

12. Tveden-Nyborg P, Bergmann TK, Jessen N, Simonsen U, Lykkesfeldt J. BCPT policy for experimental and clinical studies. Basic & clinical pharmacology & toxicology. 2021;128:4-8.

13. Nirogi R, Kandikere V, Mudigonda K, Bhyrapuneni G, Muddana N, Saralaya R, et al. A simple and rapid method to collect the cerebrospinal fluid of rats and its application for the assessment of drug penetration into the central nervous system. J Neurosci Methods. 2009;178:116-9.

14. Liu M, Zhu D, Wen J, Ding W, Huang S, Xia C, et al. Berberine Promotes OATP1B1 Expression and Rosuvastatin Uptake by Inducing Nuclear Translocation of FXR and LXRalpha. Frontiers in pharmacology. 2020;11:375.

15. Saeedi Saravi SS, Saeedi Saravi SS, Arefidoust A, Dehpour AR. The beneficial effects of HMG-CoA reductase inhibitors in the processes of neurodegeneration. Metabolic brain disease. 2017;32:949-65.

16. Ghittoni R, Lazzerini PE, Pasini FL, Baldari CT. T lymphocytes as targets of statins: molecular mechanisms and therapeutic perspectives. Inflammation & allergy drug targets. 2007;6:3-16.

17. Wood WG, Eckert GP, Igbavboa U, Müller WE. Statins and neuroprotection: a prescription to move the field forward. Annals of the New York Academy of Sciences. 2010;1199:69-76.

18. Kristof RA, Grimm JM, Stoffel-Wagner B. Cerebrospinal fluid leakage into the subdural space: possible influence on the pathogenesis and recurrence frequency of chronic subdural hematoma and subdural hygroma. Journal of neurosurgery. 2008;108:275-80.

19. Edlmann E, Giorgi-Coll S, Whitfield PC, Carpenter KLH, Hutchinson PJ. Pathophysiology of chronic subdural haematoma: inflammation, angiogenesis and implications for pharmacotherapy. J Neuroinflammation. 2017;14:108.

20. Lennernäs HJCp. Clinical pharmacokinetics of atorvastatin. 2003;42:1141-60.

21. Kureishi Y, Luo Z, Shiojima I, Bialik A, Fulton D, Lefer DJ, et al. The HMG-CoA reductase inhibitor simvastatin activates the protein kinase Akt and promotes angiogenesis in normocholesterolemic animals. Nature medicine. 2000;6:1004-10.

22. Davignon J, Jacob RF, Mason RP. The antioxidant effects of statins. Coronary artery disease. 2004;15:251-8.

23. Thompson BJ, Sanchez-Covarrubias L, Slosky LM, Zhang Y, Laracuente ML, Ronaldson PT. Hypoxia/reoxygenation stress signals an increase in organic anion transporting polypeptide 1a4 (Oatp1a4) at the blood-brain barrier: relevance to CNS drug delivery. J Cereb Blood Flow Metab. 2014;34:699-707.

24. Draude G, Hrboticky N, Lorenz RL. The expression of the lectin-like oxidized low-density lipoprotein receptor (LOX-1) on human vascular smooth muscle cells and monocytes and its down-regulation by lovastatin. Biochem Pharmacol. 1999;57:383-6.

25. Neuvonen PJ, Niemi M, Backman JT. Drug interactions with lipid-lowering drugs: mechanisms and clinical relevance. Clin Pharmacol Ther. 2006;80:565-81.

26. McCune JS, Hawke RL, LeCluyse EL, Gillenwater HH, Hamilton G, Ritchie J, et al. In vivo and in vitro induction of human cytochrome P4503A4 by dexamethasone. Clin Pharmacol Ther. 2000;68:356-66.

27. Alam K, Crowe A, Wang X, Zhang P, Ding K, Li L, et al. Regulation of Organic Anion Transporting Polypeptides (OATP) 1B1- and OATP1B3-Mediated Transport: An Updated Review in the Context of OATP-Mediated Drug-Drug Interactions. International journal of molecular sciences. 2018;19.

Posted on 5 Dec 2022 — The copyright holder is the author/funder. All rights reserved. No reuse without permission. — https://doi.org/10.22541/au.167024883.31459211/v1 — This a preprint and has not been peer reviewed. Data may be preliminary.

28. Yao HT, Hsu YR, Li ML. Beverage-Drug Interaction: Effects of Green Tea Beverage Consumption on Atorvastatin Metabolism and Membrane Transporters in the Small Intestine and Liver of Rats. Membranes (Basel). 2020;10.

29. Huang W, Zhou J, Zhang G, Zhang Y, Wang H. Decreased H3K9 acetylation level of LXRα mediated dexamethasone-induced placental cholesterol transport dysfunction. Biochimica et biophysica acta Molecular and cell biology of lipids. 2019;1864:158524.

Table 1. Standard curve and correlation coefficient of ATV and its metabolites in plasma

Analyte	Standard curve	Correlation coefficient
ATV	Y = 0.1914X + 0.0063	r^2=0.9969
o-ATV	Y = 0.3444X - 0.0089	r^2=0.9939
p-ATV	Y = 0.2653X - 0.0005	r^2 = 0.9968

Abbreviations: ATV, atorvastatin; *o*- ATV, *o*- hydroxy atorvastatin; *p*- ATV, *p*- hydroxy atorvastatin.

Table 2. The intra- and inter-batch precision and accuracy of ATV,*o*- ATV, and *p*- ATV in rat plasma (intra-batch, n=5; inter-batch, n=6)

Analyte	Added concentration (ng/ml)	Intra-batch	Intra-batch	Intra-batch	Inter-batch
		Found (mean±SD, ng/mL)	RSD (%)	RE (%)	Found (mean±SD, ng/
ATV	1	1.02 ±0.07	6.49%	2.46%	1.02±0.04
	5	4.90 ±0.26	5.38%	-1.98%	4.49 ±0.07
	12	12.51 ±1.62	12.97%	4.25%	11.95 ±1.14
o-ATV	1	1.02 ±0.11	10.45%	1.67%	1.02 ±0.05
	5	5.24 ±0.56	10.63%	4.81%	5.35 ±0.50
	12	12.75 ±1.64	12.84%	6.28%	12.28 ±0.01
p-ATV	0.5	0.45 ±0.05	10.35%	-9.41%	0.45 ±0.05
	1	0.94 ±0.13	14.36%	-6.28%	1.02 ±0.09
	5	4.67 ±0.33	7.07%	-6.60%	5.56 ±0.30

Abbreviations: ATV, atorvastatin; *o*- ATV, *o*- hydroxy atorvastatin; *p*- ATV, *p*- hydroxy atorvastatin; RSD, relative standard deviation; RE, relative error; SD, standard deviation.

Table 3. Matrix effects of ATV, *o*- ATV, and *p*- ATV in rat plasma (n=5)

Analyte	Added concentration($ng \cdot mL^{-1}$)	Matrix effect
ATV	1	106.6±6.1
	12	106.6±6.5
o-ATV	1	105.3±7.4
	12	95.9±11.3
p-ATV	0.5	90.1±6.8
	5	89.8±8.9

Abbreviations: ATV, atorvastatin; *o*- ATV, *o*- hydroxy atorvastatin; *p*- ATV, *p*- hydroxy atorvastatin.

Table 4. Extraction recovery rate of ATV, *o*- ATV, *p*- ATV in rat plasma (n=5)

Posted on 5 Dec 2022 — The copyright holder is the author/funder. All rights reserved. No reuse without permission. — https://doi.org/10.22541/au.167024883.31459211/v1 — This a preprint and has not been peer reviewed. Data may be preliminary.

Analyte	Added concentration(ng·mL^{-1})	Extraction recovery
ATV	1	91.69±6.19
	5	100.82±9.02
	12	93.20±3.78
o-ATV	1	71.23±4.43
	5	70.01±4.88
	12	69.18±0.05
p-ATV	0.5	87.10±5.35
	1	77.48±5.38
	5	75.09±5.25

Abbreviations: ATV, atorvastatin; *o*- ATV, *o*- hydroxy atorvastatin; *p*- ATV, *p*- hydroxy atorvastatin.

Table 5. The stability of ATV, *o*- ATV, and *p*- ATV in rat plasma (n=5)

Analyte	Added concentration (ng·mL^{-1})	RE (%)	RE (%)	RE (%)	RE (%
		Room temperature (25)4h	Autosampler (10)24h	4refrigerator 24h	-20refri
ATV	1	99.4±7.6	102.0±18.6	107.0±6.4	102.1±
	12	106.6±12.0	96.9±10.6	99.2±6.6	105.3±
o-ATV	1	97.2±8.2	106.0±14.8	97.5±9.2	106.9±
	12	96.0±9.8	108.9±10.3	107.0±8.9	111.0±
p-ATV	0.5	108.1±2.6	98.1±6.2	99.1±3.2	98.0±1
	2.5	101.9±6.8	102.8±8.8	102.2±10.2	98.8±9

Abbreviations: ATV, atorvastatin; *o*- ATV, *o*- hydroxy atorvastatin; *p*- ATV, *p*- hydroxy atorvastatin; RE, relative error.

Table 6. Pharmacokinetic parameters of ATV, o-ATV, p-ATV

Drug	**Parameter**	**ATV**	**ATV+DXM**	**GMR (90%CI)**
ATV	C_{max} (ng/mL)	23.565±9.41	27.6±8.605*	1.388 (0.774-2.003)
	$AUC_{(0\text{-}t)}$ (ng·h/mL)	51.785±16.625	105.939±37.474*	2.156 (1.495-2.817)
	$AUC_{(0\text{-}[?])}$ (ng·h/mL)	59.007±20.732	143.022±55.368*	2.550 (1.777-3.324)
	t_{max} (h)	1 (0.58-1)	0.42 (0.25-3)	——
	$t_{1/2}$ (h)	5.379±2.242	16.476±18.848*	2.304 (1.128-4.707)
***o*-ATV**	C_{max} (ng/mL)	36.688±10.381	36.478±17.13	1.313 (0.475-2.152)
	$AUC_{(0\text{-}t)}$ (ng·h/mL)	109.793±40.675	242.318±95.706*	2.320 (1.671-2.969)
	$AUC_{(0\text{-}[?])}$ (ng·h/mL)	112.6±41.404	257.492±87.942*	2.420 (1.800-3.004)
	t_{max} (h)	1.75 (1-3)	1.25 (0.25-2)	——
	$t_{1/2}$ (h)	2.627±1.01	5.73±2.261*	2.196(1.421-3.394)
***p*-ATV**	C_{max} (ng/mL)	4.082±1.807	4.062±1.544	1.106 (0.706-1.505)
	$AUC_{(0\text{-}t)}$ (ng·h/mL)	16.905±7.234	36.331±12.913*	2.209 (2.034-2.384)
	$AUC_{(0\text{-}[?])}$ (ng·h/mL)	18.038±7.577	45.02±13.478*	2.676 (1.908-3.443)
	t_{max} (h)	1.5 (0.58-12)	1.5 (1-12)	——
	$t_{1/2}$ (h)	4.17±1.821	10.349±5.325*	2.457(1.565-3.857)

Abbreviations: ATV, atorvastatin; *o*- ATV, *o*- hydroxy atorvastatin; *p*- ATV, *p*- hydroxy atorvastatin; C_{max}, peak plasma concentration; $AUC_{(0\text{-}t)}$, area under plasma concentration-time curve from time 0 to 24 hours;

AUC $_{(0\text{-}[?])}$, area under plasma concentration-time curve from time 0 to infinity; t_{max}, time to peak plasma concentration; $t_{1/2}$, elimination half-life; GMR, geometric mean ratios; CI, confidence intervals.

Note: Values are shown as mean ± SD unless otherwise indicated; * Significantly different from the ATV group, $P < 0.05$.

Figure legends

Figure 1. The representative chromatograms of ATV (A),*o*- ATV (B), *p*- ATV (C), d5-ATV (D), and RSV (E) in rat plasma. Abbreviations: ATV, atorvastatin; *o*- ATV, *o*- hydroxy atorvastatin;*p*- ATV, *p*- hydroxy atorvastatin; d5-ATV, d5-atorvastatin; RSV, rosuvastatin.

Figure 2. Plasma concentration-time profiles of ATV (A),*o*- ATV (B), and *p*- ATV (C) in rat plasma. Atorvastatin calcium (0.27 mg/100 g) and dexamethasone acetate (0.02 mg/100 g) were orally administered to rats for a single dose. Values at each time point are expressed as the mean ± SD (n = 6). Abbreviations: ATV, atorvastatin; *o*- ATV, *o*- hydroxy atorvastatin;*p*- ATV, *p*- hydroxy atorvastatin.

Figure 3. The concentration of ATV in plasma and CSF.

A: Valley concentration of ATV in plasma and CSF (n = 8). ATV (PLASMA vs CSF, Unpaired t-test, $^{**}P = 0.0060$), ATV+DXM (PLASMA vs CSF, Mann-Whitney U test, $^{*}P = 0.0200$), PLASMA (ATV vs ATV+DXM, Unpaired t-test, $P = 0.3213$); B: Peak concentration of ATV in plasma and CSF (n = 5). ATV (PLASMA vs CSF, Mann-Whitney U test, $^{**}P = 0.0079$), ATV+DXM (PLASMA vs CSF, Unpaired t test, $^{*}P = 0.0150$), PLASMA (ATV vs ATV+DXM, Unpaired t test, $^{*}P = 0.0275$). The values are given as mean ± SD. Abbreviations: ATV, atorvastatin; DXM dexamethasone; CSF, cerebrospinal fluid.

Figure 4. DXM inhibited the expression of OATP1B1 and LXRα in rat liver.

A: Expressions of OATP1B1 were analyzed by Western blot assay; B: The protein expression quantification of OATP1B1 (Tukey's multiple comparisons test, Control vs. DXM, $^{*}P = 0.0436$; ATV vs. ATV+DXM, $^{**}P = 0.0066$); C: Expressions of LXRα was analyzed by Western blot assay; D: The protein expression quantification of LXRα (Tukey's multiple comparisons test, Control vs. DXM, $^{***}P = 0.0005$; ATV vs. ATV+DXM, $^{**}P = 0.0038$). The values are given as mean ± SD (n = 6). Abbreviations: ATV, atorvastatin; DXM dexamethasone; OATP1B1, organic anion transporting polypeptides 1B1; LXRα, liver X receptor α.

Figure 5. DXM decreased the ATV uptake and inhibited OATP1B1 and LXRα expressions in HepG2 cells. A: Cytotoxicity of 100 nM ATV and 400 nM DXM on HepG2 cells was measured using the Cell Counting kit-8; B: The uptake of ATV by HepG2 cells after treated with 400 nM DXM (Unpaired t-test, ATV vs. ATV+DXM, $^{**}P = 0.0011$); C: OATP1B1 and LXRα expressions were analyzed by Western blot assay; D: The protein expression quantification of OATP1B1 (Tukey's multiple comparisons test, ATV vs. DXM, $^{*}P = 0.0262$; ATV vs. ATV+DXM, $^{*}P = 0.0339$); E: The protein expression quantification of LXRα (Tukey's multiple comparisons test, Control vs. DXM, $^{*}P = 0.0167$; ATV vs. ATV+DXM, $^{*}P = 0.0290$). The values are given as mean ± SD (n = 3). Abbreviations: ATV, atorvastatin; DXM dexamethasone; OATP1B1, organic anion transporting polypeptides 1B1; LXRα, liver X receptor α.

Figure 6. DXM inhibited OATP1B1 promoter activation via LXRα. Renilla reporter activity was used as an internal control. Values were normalized for those in the empty plasmid transfected cells and were expressed relative to that in the control. (one-way ANOVA, 0.1%DMSO vs. GW3965, $^{****}P < 0.0001$; 0.1%DMSO vs. DXM, $^{***}P = 0.0003$; GW3965 vs. DXM+GW3965, $^{****}P < 0.0001$). The values are given as mean ± SD (n = 3). Abbreviations: DXM dexamethasone; OATP1B1, organic anion transporting polypeptides 1B1; LXRα, liver X receptor α· GW3965, LXRα agonist.

Posted on 5 Dec 2022 — The copyright holder is the author/funder. All rights reserved. No reuse without permission. — https://doi.org/10.22541/au.167024883.31459211/v1 — This a preprint and has not been peer reviewed. Data may be preliminary.

Posted on 5 Dec 2022 — The copyright holder is the author/funder. All rights reserved. No reuse without permission. — https://doi.org/10.22541/au.167024883.31459211/v1 — This a preprint and has not been peer reviewed. Data may be preliminary.

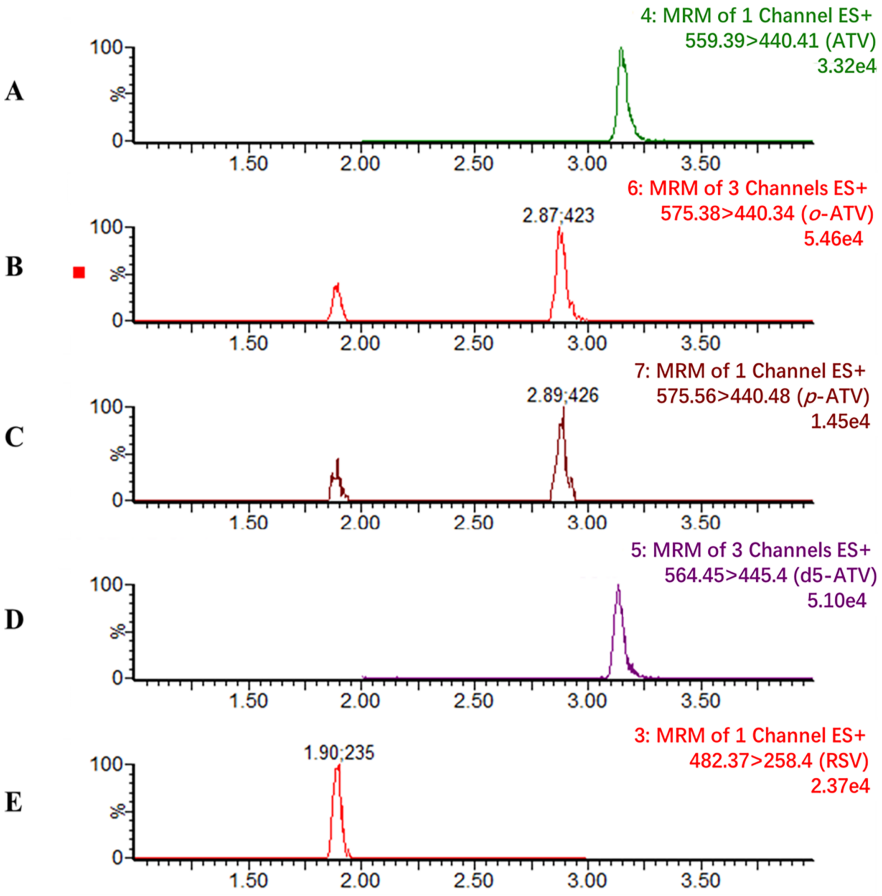

Posted on 5 Dec 2022 — The copyright holder is the author/funder. All rights reserved. No reuse without permission. — https://doi.org/10.22541/au.167024883.31459211/v1 — This a preprint and has not been peer reviewed. Data may be preliminary.

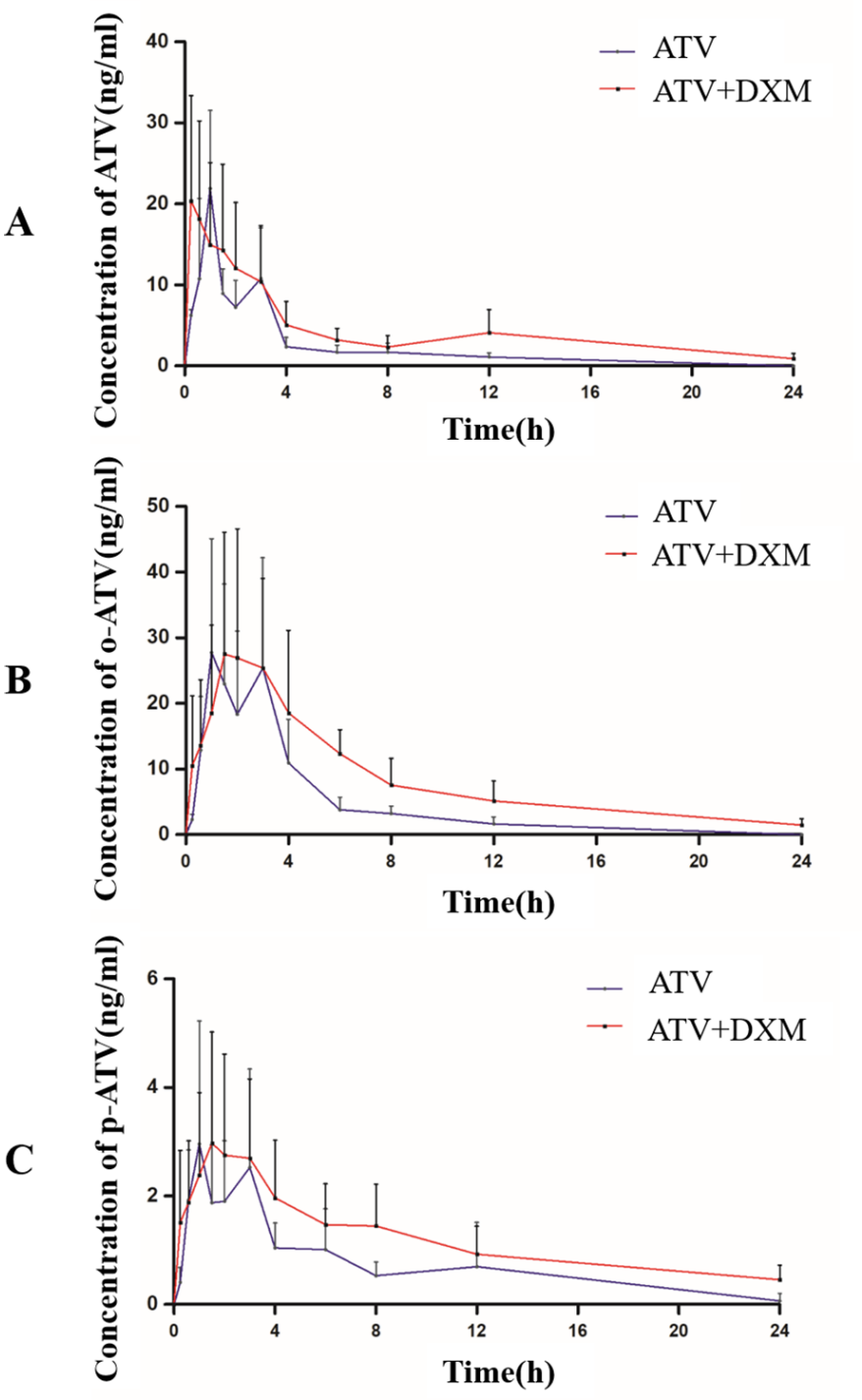

Posted on 5 Dec 2022 — The copyright holder is the author/funder. All rights reserved. No reuse without permission. — https://doi.org/10.22541/au.167024883.31459211/v1 — This a preprint and has not been peer reviewed. Data may be preliminary.

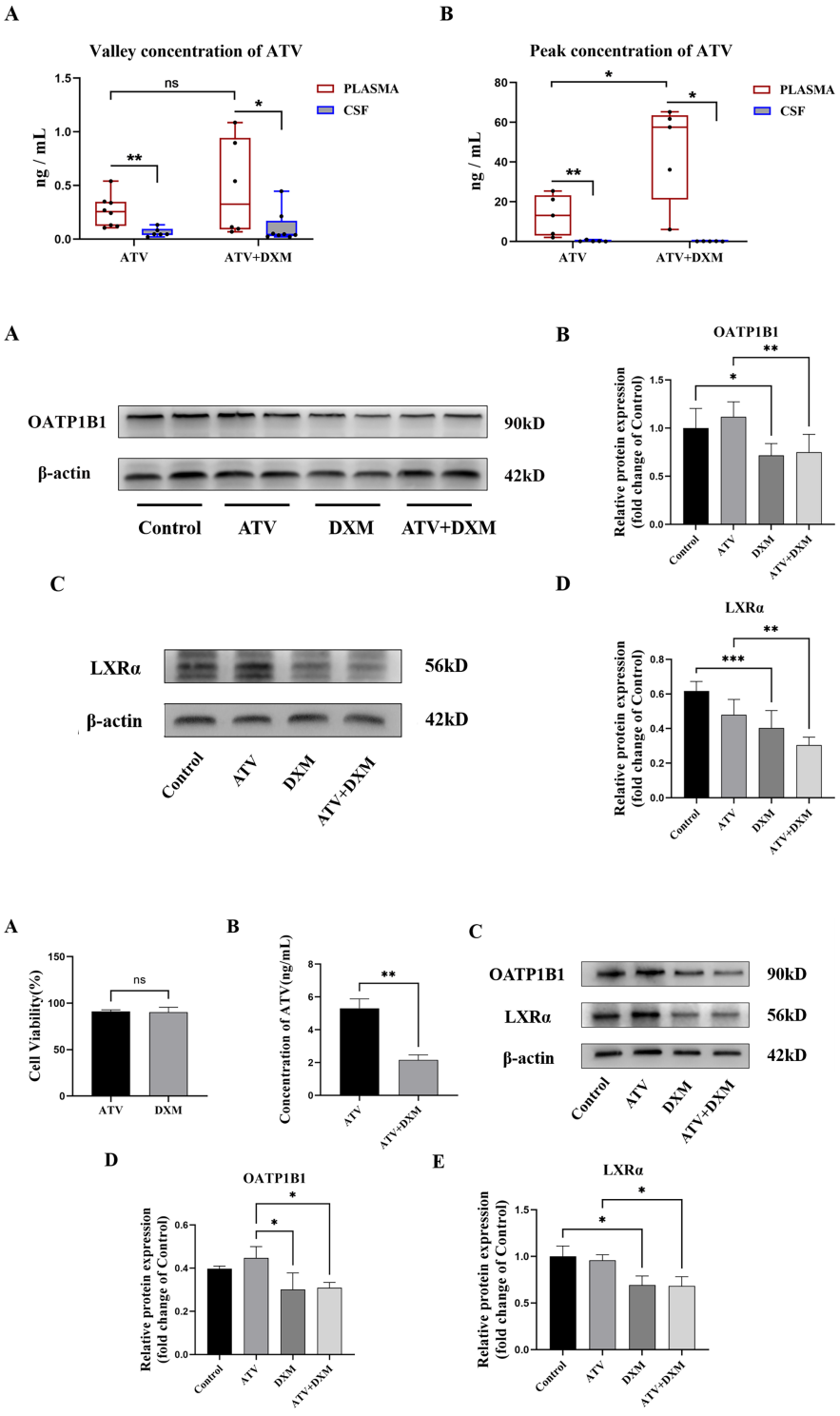

Posted on 5 Dec 2022 — The copyright holder is the author/funder. All rights reserved. No reuse without permission. — https://doi.org/10.22541/au.167024883.31459211/v1 — This a preprint and has not been peer reviewed. Data may be preliminary.